J|A|C|S
COMMUNICATIONS

Published on Web 08/22/2006

Monodisperse Lanthanide Oxysulfide Nanocrystals

Fei Zhao, Mei Yuan, Wen Zhang, and Song Gao*

Beijing National Laboratory for Molecular Sciences, State Key Laboratory of Rare Earth Materials Chemistry and Applications, College of Chemistry and Molecular Engineering, Peking University, Beijing 100871, China

Received June 1, 2006; E-mail: gaosong@pku.edu.cn

Lanthanide compounds have long been recognized for their promising applications in various fields based on the electronic, magnetic, optical, and chemical characteristics arising from their f electrons.[1] Also, lanthanide oxysulfides M_2O_2S (M = La−Lu) received particular attention due to their high performance as fluorescence materials. In addition, they have significant commercial applications, such as in radiation intensifying screens, X-ray-computed tomography, oxygen storage, and medical imaging radiation detectors.[2] More recently, many efforts were stimulated toward the design and synthesis of lanthanide oxides, chalcogenides, and fluorides at the nanoscale due to their interesting properties that differ from those of the bulk materials.[3] Although a few M_2O_2S nanomaterials have been produced,[4] the synthesis of monodisperse M_2O_2S nanocrystals still remains a challenge for researchers to date because of the great difficulty in finding an effective synthetic route. Herein, we developed a facile colloidal synthesis of M_2O_2S short nanorods and monodisperse nanoplates with thickness as small as ca. 1.65 nm.

Colloidal nanocrystals have attracted growing interest for both their fundamental size- and shape-dependent properties and their self-assembly potential for device and biomedical applications.[5] The thermal decomposition of molecular precursors is an effective method to synthesize colloidal nanoscale metals/alloys and metallic chalcogenides, including ternary compounds.[6] The conventional synthetic processes were usually carried out under a flow of protective atmosphere. Few studies were performed on the open reaction system directly exposed to air. In our previous work, monodisperse EuS nanocrystals were synthesized by the thermal decomposition of the single precursors [Eu(phen)(ddtc)$_3$] (phen = 1,10-phenanthroline; ddtc = diethyldithiocarbamate) under a flow of nitrogen.[7] Here we obtained Eu_2O_2S nanocrystals by using the same precursors in the absence of protective conditions. The oxygen in the air acts as the oxidant during the nucleation and growth course of colloidal M_2O_2S nanocrystals. Compared with the previous methods for preparing lanthanide oxysulfides,[2,4] our synthetic conditions were mild, and the morphology of the products could be easily controlled by selecting appropriate surfactants. When oleylamine/oleic acid/octadecene (OM/OA/ODE) were used as mixed solvents and surfactants, we obtained Eu_2O_2S nanoplates (see Scheme S1 and detailed synthetic procedure in Supporting Information). The use of solvent OM as well as a single stabilizer led to the formation of short nanorods.

The shape, size, lattice structure, and self-arrangement of the Eu_2O_2S nanostructures were characterized by transmission electron microscopy (TEM, Philips Tecnai F30FEG-TEM, 300 kV). As demonstrated in Figure 1a, the synthesized Eu_2O_2S hexagonal nanoplates possess a relatively uniform thickness of 1.65 nm and self-assemble face-to-face into nanowires with lengths more than 5 μm (see Figure S1) when the products were dissolved in mixed solvents of toluene/ethanol. Figure 1b and the inset present a single separated nanowire. According to the high-resolution TEM (HRTEM) shown in Figure 1c, the growth along the {002} facets

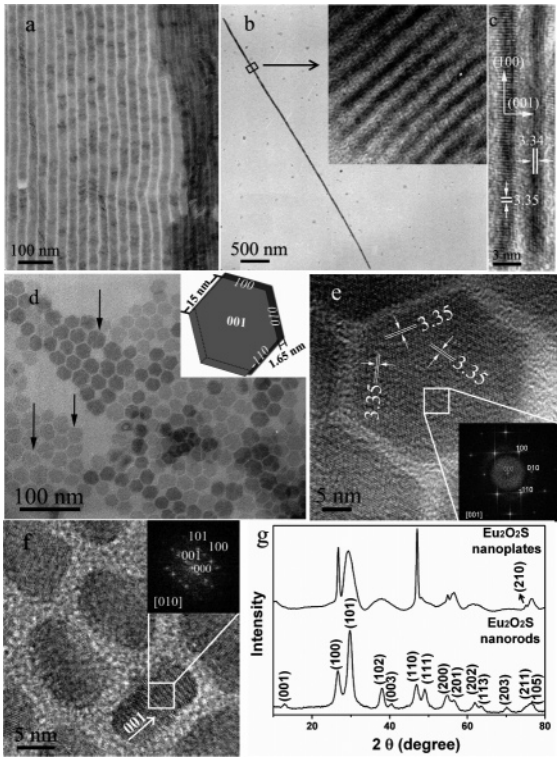

Figure 1. (a) TEM images of superlattice arrays of Eu_2O_2S nanoplates. (b) TEM images of a nanoplate self-assembled to a single nanowire. (c) HRTEM images of the nanoplates standing on the surface. (d) TEM images of the nanoplates lying flat on the surface (inset: a schematic diagram of a hexagonal nanoplate). (e) HRTEM image of Eu_2O_2S nanoplates lying flat on the face (inset: FFT of the border region). (f) HRTEM image of Eu_2O_2S short nanorods (inset: FFT). (g) Powder XRD patterns.

of the hexangular structure with an interplanar distance of 0.334 nm is strongly restricted. Figure 1d shows the nanoplates, taken from their solution in toluene, lying flat on the TEM grid with a side dimension of 15 nm. Some of the nanoplates were found broken (guided by the arrows) because of the brittle character of their ultrathin structures. Figure 1e reveals an interplanar spacing of 0.335 nm along the [100] direction. Fast Fourier transform (FFT) pattern of the border region (inset of Figure 1e) reveals the hexagonal structure projected from the [001] direction. These indicate that the {100} planes are parallel to the edge of hexagonal plates. The energy-dispersive X-ray spectroscopy (EDX) results also prove the formation of Eu_2O_2S nanocrystals (see Figure S2). Figure S3a shows the TEM image of Eu_2O_2S short nanorods with dimensions of 6.5 ± 1.0 nm × 10 ± 1.5 nm in addition to a small fraction of nanoparticles. HRTEM image, as given in Figure 1f (inset is FFT of the border region), shows that the nanorods grow along the [001] direction. Electron microdiffraction (ED) pattern (Figure S3b) reveals the well crystalline nature of these nanorods.

10.1021/ja0638410 CCC: $33.50

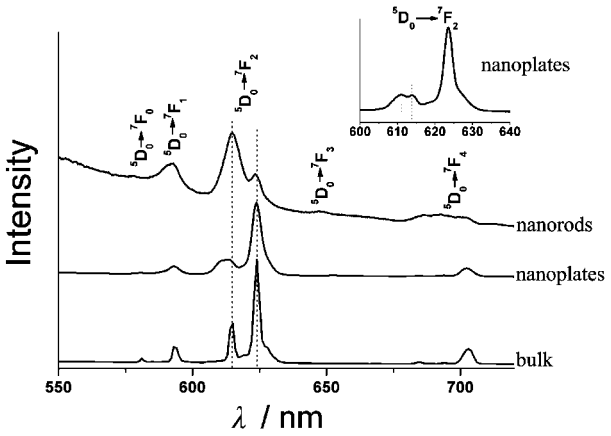

Figure 2. Room temperature fluorescence emission spectra (Hitachi F-4500) of Eu_2O_2S nanoplates with a side dimension of 15 nm and a thickness of 1.65 nm (λ_{ex} = 306 nm), nanorods (λ_{ex} = 300 nm), and bulk Eu_2O_2S (λ_{ex} = 262 nm). The inset indicates the splitting of the peak at 614 nm.

The typical X-ray diffractions (XRD) of the as-obtained nanoplates and nanorods are shown in Figure 1g. All Bragg reflections can be well indexed with space group $P\bar{3}m1$ and cell constants a = 3.868 and c = 6.685, which are close to the reported data for pure Eu_2O_2S phase (JCPDS card file: 26-1418). For Eu_2O_2S nanoplates, the (100) and (110) reflections show narrower peak widths than the other ones due to their anisotropic structures and critical dimensions on the order of nanometers.

The surfactants adsorb to the nanocrystal surface and control growth by providing steric stabilization and preventing aggregation. Materials with anisotropic crystal structure, such as Eu_2O_2S hexagonal materials, are predisposed to anisotropic growth since the {001} planes exhibit significantly different surface energies relative to the {100} and {110} crystal planes (see the crystal views of the Eu_2O_2S in Figure S4).[8] It has been reported that alkylamines often bind weakly to the metal centers on the surface of nanocrystals and, in particular, less strongly than carboxylic acids of the same carbon chain length (see Figure S5).[9] When OM was used as single solvent and stabilizer, the Eu_2O_2S nuclei will grow in a 3D mode to generate short nanorods. OA is necessary in the synthesis of nanoplates. The facet of {001} with a higher density of Ln^{3+} is easy to be passivated by the adsorption of OA, and the growing of this facet is restricted. The dimensions of the nanoplates can be modulated by controlling the reaction temperature, the concentration of monomer, and the addition ratio of stabilizers OA/OM (see Figure S6). Gd_2O_2S and Sm_2O_2S nanoplates were also obtained by the decomposition of the corresponding precursors (see Figures S7−S9).

The emission spectra of Eu_2O_2S nanoplates, nanorods, and bulk Eu_2O_2S are shown in Figure 2 (see XRD pattern for bulk Eu_2O_2S in Figure S10). The main emission peaks are ascribed to Eu^{3+} transition from ^5D_J (J = 0, 1) to ^7F_J (J = 0−4). The emission spectrum was broadened, and the intensity ratio of the peak at 614 nm to the peak at 623 nm was obviously enhanced for the sample of the Eu_2O_2S nanorods compared with that of the bulk sample. In the case of Eu_2O_2S nanoplates, the peak at 614 nm split into two obvious peaks of 611 and 614 nm. The lower crystal field symmetry at the surface is considered to be the main origin of these unusual behaviors. Eu^{3+} is a non-Kramers' ion, and its electronic J-level degeneracy can be destroyed by a low symmetry crystal field interaction. Thus we found the degenerated line split and the spectrum broadened.[10] Gd_2O_2S:Eu nanoplates show luminescent properties similar to those of Eu_2O_2S nanoplates, while they exhibit a stronger emission intensity (Figures S11 and S12). The photoluminescent quantum yields (QYs) of the as-prepared Eu^{3+}-doped Gd_2O_2S nanoplates were determined to be 3.6, 1.1, and 0.9% for Gd_2O_2S:Eu (1%), Gd_2O_2S:Eu (5%), and Gd_2O_2S:Eu (15%), respectively (see Supporting Information). These values are lower than the QYs of the bulk lanthanide oxysulfide phosphors, probably because of the drastically enlarged surface-to-volume ratio favoring recombination, which does not engender visible emission.[11]

In conclusion, we have successfully synthesized monodisperse europium oxysulfide nanoplates by thermally decomposing the molecular precursors when exposing the reactants to air. The Eu_2O_2S nanoplates could be modulated in dimensions, and these as-synthesized nanoplates could self-assemble into superlattice arrays. The unusual luminescence properties differing from the bulk powder phosphors result from the surface-modification effects. These results provide an effective route to synthesize M_2O_2S nanocrystals and are helpful for investigating the optic characters in the nanostructures, and promote the potential biomedical applications of M_2O_2S nanocrystals.

Acknowledgment. We are grateful to Prof. W. F. Fu, Dr. C. J. Jia, Y. Chen, and X. J. Zhao for their kind help. We thank the NSFC (20221101, 20490210) and the National Basic Research Program of China (2006CB601102) for financial support.

Supporting Information Available: Detailed synthetic method and characterization. More TEM, SEM images, XRD, EDX patterns, emission spectra of Gd_2O_2S:Eu. This material is available free of charge via the Internet at http://pubs.acs.org.

References

(1) Wachter, P. *Handbook on the Physics and Chemistry of Rare Earths*, 2nd ed.; North-Holland Publishing Company: Amsterdam, 1979.
(2) (a) Yu, S. H.; Han, Z. H.; Yang, J.; Zhao, H. Q.; Yang, R. Y.; Xie, Y.; Qian, Y. T.; Zhang, Y. H. *Chem. Mater.* **1999**, *11*, 192. (b) Machida, M.; Kawamura, K.; Ito, K.; Ikeue, K. *Chem. Mater.* **2005**, *17*, 1487. (c) Toki, H.; Ito, S. *Jpn. Kokai Tokkyo Koho* JP 08 64, 147. (d) Cavouras, D.; Kandarakis, I.; Maris, T.; Panayiotakis, G. S.; Nomicos, C. D. *Eur. J. Radio.* **2000**, *35*, 70. (e) da Vila, L. D.; Stucchi, E. B.; Davolos, M. R. *J. Mater. Chem.* **1997**, *7*, 2113.
(3) (a) Cao, Y. C. *J. Am. Chem. Soc.* **2004**, *126*, 7456. (b) Wang, X.; Li, Y. D. *Angew. Chem., Int. Ed.* **2003**, *42*, 3497. (c) Si, R.; Zhang, Y. W.; You, L. P.; Yan, C. H. *Angew. Chem., Int. Ed.* **2005**, *44*, 3256. (d) Zhang, Y. W.; Sun, X.; Si, R.; You, L. P.; Yan, C. H. *J. Am. Chem. Soc.* **2005**, *127*, 3260. (e) Yu, T.; Joo, J.; Park, Y. I.; Hyeon, T. *Angew. Chem., Int. Ed.* **2005**, *44*, 7411. (f) Yu, T.; Joo, J.; Park, Y. I.; Hyeon, T. *J. Am. Chem. Soc.* **2006**, *128*, 1786. (g) Mirkovic, T.; Hines, M. A.; Nair, P. S.; Scholes G. D. *Chem. Mater.* **2005**, *17*, 3451.
(4) Dhanaraj, J.; Jagannathan, R.; Trivedi, D. C. *J. Mater. Chem.* **2003**, *13*, 1778.
(5) (a) Alivisatos, A. P. *Science* **1996**, *271*, 933. (b) Park, J.; An, K.; Hwang, Y.; Park, J. G.; Noh, H. J.; Kim, J. Y.; Park, J. H.; Hwang, N. M.; Hyeon, T. *Nat. Mater.* **2004**, *3*, 891. (c) Sun, S. H. *Adv. Mater.* **2006**, *18*, 393. (d) Cademartiri, L.; Bertolotti, J.; Sapienza, R.; Wiersma, D. S.; Freymann, G.; Ozin, G. A. *J. Phys. Chem. B* **2006**, *110*, 671.
(6) (a) Ng, M. T.; Boothroyd, C. B.; Vittal, J. J. *J. Am. Chem. Soc.* **2006**, *128*, 7118. (b) Gou, X. L.; Cheng, F. Y.; Shi, Y. H.; Zhang, L.; Peng, S. J.; Chen, J.; Shen, P. W. *J. Am. Chem. Soc.* **2006**, *128*, 7222.
(7) Zhao, F.; Sun, H. L.; Su, G.; Gao, S. *Small* **2006**, *2*, 244.
(8) (a) Larsen, T. H.; Sigman, M.; Ghezelbash, A.; Doty, R. C.; Korgel, B. A. *J. Am. Chem. Soc.* **2003**, *125*, 16050. (b) Zhang, H. T.; Wu, G.; Chen, X. H. *Langmuir* **2003**, *19*, 4281.
(9) (a) Cheon, J.; Kang, N.-J.; Lee, S.-M.; Lee, J.-H.; Yoom, J.-H.; Oh, S. J. *J. Am. Chem. Soc.* **2004**, *126*, 1950. (b) Casula, M. F.; Jun, Y.-W.; Zaziski, D. J.; Chan, E. M.; Corrias, A.; Alivisatos, A. P. *J. Am. Chem. Soc.* **2006**, *128*, 1675.
(10) Yan, C. H.; Sun, L. D.; Liao, C. S.; Zhang, Y. X.; Lu, Y. Q.; Huang, S. H.; Lu, S. Z. *Appl. Phys. Lett.* **2003**, *82*, 3511.
(11) (a) Wang, H. Z.; Uehara, M.; Nakamura, H.; Miyazaki, M.; Maeda, H. *Adv. Mater.* **2005**, *17*, 2506. (b) Riwotzki, K.; Haase, M. *J. Phys. Chem. B* **2001**, *105*, 12709.

JA0638410